Journal of
Materials Chemistry A

Accepted Manuscript

This article can be cited before page numbers have been issued, to do this please use: W. L. Yang, M. H. Zhou, J. J. Cai, L. Liang, G. B. Ren and L. Jiang, *J. Mater. Chem. A*, 2017, DOI: 10.1039/C7TA01534H.

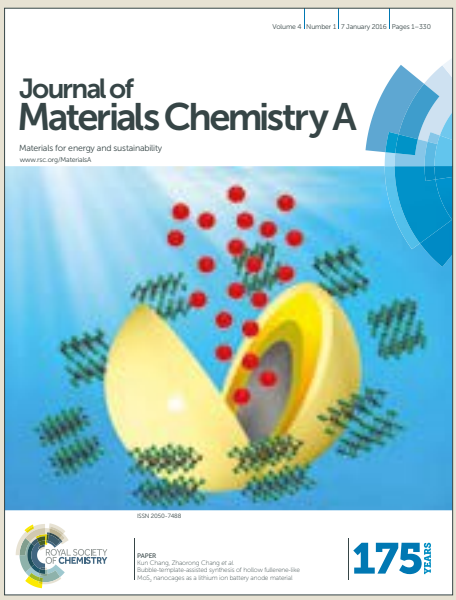

ROYAL SOCIETY OF CHEMISTRY

rsc.li/materials-a

View Article Online
DOI: 10.1039/C7TA01534H

Ultrahigh yield of hydrogen peroxide on graphite felt cathode modified with electrochemically exfoliated graphene

Weilu Yang[a,b], Minghua Zhou[a,b,*], Jingju Cai[a,b], Liang Liang[a,b], Gengbo Ren[a,b], Lili Jiang[a,b]

[a] *Key Laboratory of Pollution Process and Environmental Criteria, Ministry of Education, College of Environmental Science and Engineering, Nankai University, Tianjin 300071, China*

[b] *Tianjin Key Laboratory of Urban Ecology Environmental Remediation and Pollution Control, College of Environmental Science and Engineering, Nankai University, Tianjin 300071, China*

[*] Corresponding author. Tel./Fax: +86 22 23501117; E-mail: zhoumh@nankai.edu.cn (M. Zhou).

View Article Online
DOI: 10.1039/C7TA01534H

Abstract:

The development of efficient oxygen reduction reaction (ORR) cathode for hydrogen peroxide production represents an important challenge in the field of electrochemical processes and is highly demanded for chemical industries and environmental remediation application. In this work, a novel graphite felt cathode modified with electrochemically exfoliated graphene (EEGr) and carbon black was developed, presenting a very high H_2O_2 generation rate of 7.7 mg h^{-1} cm^{-2} with relatively low energy consumption (9.7 kWh kg^{-1}). Characterized by SEM, TEM, AFM, Raman, XRD and XPS, the synthesized EEGr was proved to be the 3-4 layers thin sheet with low defects. Important cathode manufacture parameters including the ratio and loading of EEGr were optimized, and the dependence of H_2O_2 generation with pH and cathode potential as well as performance stability were investigated. At optimized cathode potential -0.9 V and pH 7, the modified cathode kept stable performance for H_2O_2 generation during 10 cycles, which was 2 times of the cathode without EEGr. Further explored by CV, rotating disk electrode (RDE) and contact angles analysis, the presence of EEGr was found to accelerate electrons transfer rate, benefit oxygen surface reaction, but not change two-electrons ORR number, which contributed to the enhanced performance for H_2O_2 production and possible mechanism was suggested. Finally, such graphene modified cathode demonstrated effectiveness for the degradation of four kinds of representative pollutants (Orange II, methylene blue, phenol and sulfadiazine) by electro-Fenton process, proving great potential practical application for organic wastewater treatment.

View Article Online
DOI: 10.1039/C7TA01534H

Introduction

Hydrogen peroxide is highly desirable and important for many manufacturing industries such as chemicals and paper-making as well as environmental remediation since it is a versatile and environmentally friendly oxidizing agent without generation of hazardous residues upon decomposition, only oxygen and water. However, the traditional process of anthraquinone oxidation, which is a multistep process to extract H_2O_2 from organic agents, is not regarded as a green method.[1] Thus the development of efficient method represents an important challenge, and significant efforts have been made either to reduce its synthesis cost,[2,3] or expand its application fields including environmental remediation.[4]

In the latter field, recent years, electro-Fenton, which combines with ferrous ion addition and the in-situ electrochemically generated H_2O_2 (eq.1) has attracted much concern for its advantages such as easy-controlling, high efficiency and environmental compatibility due to the formation of highly powerful hydroxyl radicals (•OH) (eq.2).[5]

$$O_2 + 2H^+ + 2e^- \rightarrow H_2O_2 \quad (1)$$

$$Fe^{2+} + H_2O_2 \rightarrow Fe^{3+} + OH^- + {}^{\bullet}OH \quad (2)$$

A high yield of H_2O_2 was prerequisite for the high efficiency of electro-Fenton. Various cathode materials have been widely attempted such as active carbon, carbon fiber,[6] graphite felt,[7-9] carbon black,[10] carbon nanotubes,[11] graphite carbon[12] and graphene,[5,13,14]. As a commercially available material, graphite felt is regarded as one

View Article Online
DOI: 10.1039/C7TA01534H

of the most widely used cathodes due to its large active surface and mechanical integrity, but still the yield of H_2O_2 production is not satisfying, and extensive efforts via chemical, electrochemical oxidation or acidic treatment have been made.[9] Particularly, in our previous work, the graphite felt modified with carbon black could dramatically improve the H_2O_2 generation rate up to 10 times (about 2.2 mg h^{-1} cm^{-2}) when comparing with the pristine one.[15]

Recent years, as a new carbonaceous material, graphene, which is a two-dimensional, one atom thick sheet composed of sp^2 carbon atoms arranged in a honeycomb structure, has been used as an efficient adsorbent or catalyst for environmental application due to its outstanding electrical conductivity and high specific surface area, which have become a very hot research area.[16-18] However, very few applications using it as cathode for H_2O_2 generation have been reported,[5,19,20] and what's more, the yield of H_2O_2 is still limited and the role of graphene has not been well elucidated though these cathodes modified with graphene are supposed to improve H_2O_2 electro-generation.[20,21] For example, Xu et al. reported an average H_2O_2 generation rate of 1.03 mg h^{-1} cm^{-2} on a graphene doped gas diffusion cathode,[5] while Mousset et al. showed that it was 0.64 mg h^{-1} cm^{-2} on the 3D graphene foam.[20]

These facts indicated that graphene based cathodes for H_2O_2 production need more extensive and comprehensive studies since the synthesis of graphene and its assembly on the cathode would significantly determine the cathode characteristics. Firstly, traditional graphene synthetic methods, e.g., Hummers's method, was conventionally used for graphene synthesis, however, there are some disadvantages including

View Article Online
DOI: 10.1039/C7TA01534H

extreme experimental conditions,[22] high cost[23] and possible environmental pollution, while electrochemical exfoliation of graphite (EEGr) has been reported to be a efficient method for a high production of graphene in several hours.[22,24] It would be easier to synthesis low defect graphene, expecting better cathode characteristics for H_2O_2 generation. Secondly, the manufacture of graphene-based electrodes either with pristine graphene or use of graphene coatings over some flat substrates, till now, no attempt on three dimensional material substrates, e.g., graphite felt, has been tested. As demonstrated in our previous work,[15] it would be reasonable that a small graphene loading instead of carbon black on graphite felt would enhance the specific surface area and the conductivity of the cathode, which would further improve the performance of hydrogen peroxide production.

In this context, this work reported a novel graphene-based cathode assembly strategy for high yield of H_2O_2, using graphite felt cathode modified with carbon black and graphene derived by a fast electrochemical exfoliation from graphite foil with an expansion time dramatically reduced to 1 min. The objectives of this study were: 1) synthesis of graphene by a fast electrochemical exfoliation and its characterization, 2) assembly of graphene-based cathode and optimization of important manufacture process, 3) assessment and comparison of its properties with unmodified electrode, and to elucidate possible enhancement mechanism for H_2O_2 production, and 4) to evaluate the degradation and mineralization efficiency of four kinds of model pollutants by electro-Fenton. This modified cathode exhibited a very high H_2O_2 generation rate with relatively low energy consumption, opening up a new

View Article Online
DOI: 10.1039/C7TA01534H

avenue for developing efficient graphene-based cathode for electro-Fenton.

Experimental

EEGr synthesis

Before electrochemical exfoliation, the graphite foils were soaked in ethanol with ultrasonic treatment for 30 min, then they were dried 24 h for ready. EEGr was electrochemically exfoliated in a beaker system with aqueous electrolyte containing 2 mL concentrated H_2SO_4, 10 mL KOH and 100 mL deionized water, using platinum foil sheet (1×1 cm^2) and graphite foil (2×4 cm^2) as the cathode and anode, respectively. Firstly, a bias potential of 2.5 V was applied for 1 min of expansion time, and then, the applied bias potential was increased to 10 V for about 3-5 mins. Subsequently, the exfoliated graphene sheets were filtrated with 0.22 μm membrane, and then these collected graphene flakes were dispersed into N,N-Dimethylformamide (DMF) solution with 5 min sonication. Finally, after vacuum filtration with deionized water to remove DMF, they were put into a vacuum dryer for 1 day.

Cathode modification with EEGr and carbon black

Graphite felt (2×2.5 cm^2) was used as the base cathode, carbon black and EEGr were used to modify it. With the addition of 0.14 mL PTFE, 3 mL ethanol and 2 mL dionized water, after quick shake for 15 s, a kind of seriflux was formed, which was coated onto the two sides of the graphite felt, after drying in the room temperature, the modified graphite felt electrode was annealed for 30 min at 360 °C.

View Article Online
DOI: 10.1039/C7TA01534H

The performance of the modified electrode was evaluated by the yield of H_2O_2 production and compared to the one without EEGr. The H_2O_2 electrochemical generation experiments were operated in an undivided cell in 0.05 M Na_2SO_4 (0.1 L) and with 0.7 L min^{-1} air aeration at room temperature. The modified graphite felt was selected as the cathode, and DSA (2×4 cm^2) was employed as the anode. The distance between the anode and cathode was 1 cm. At every 10 min intervals, 0.5 mL sample was taken for analyzing the concentration of H_2O_2.

The concentration of H_2O_2 was measured by the potassium titanium (IV) oxalate method at λ=400 nm with a UV-Vis spectrophotometer (UV759, Shanghai Instrument Analysis Instrument C0., Ltd). The current efficiency (CE) for the production of H_2O_2 was calculated with the following formula (3): [25]

$$CE = \frac{nFCV}{\int_0^t Idt} \times 100\% \quad (3)$$

Where n is the number of electrons transferred for oxygen reduction for H_2O_2, F is the Faraday constant (96,485 C mol^{-1}), C is the concentration of H_2O_2 production (mol L^{-1}), V is the bulk volume (L), I is the current (A), and *t* is the time of electrochemical process (s).

The electric energy consumption (EEC, kWh kg^{-1}) was measured by formula (4)[26]

$$EEC = \frac{1000UIt}{CV_s} \quad (4)$$

Where U is the applied voltage (V), I is the current (A), *t* is the time of electrochemical process (h), C is the concentration of the H_2O_2 generated (mg L^{-1}), and V_s is the solution volume (L).

View Article Online
DOI: 10.1039/C7TA01534H

Characterization and analytical methods

The morphology of EEGr was determined using scanning electron microscopy (SEM) (LEO-1530VP, Germany), transmission electron microscopy (TEM) (Titan^{TM} G2 60-300, Japan) and atomic force microscopy (AFM) (JPK NanoWizard, Germany). The Raman spectra were recorded with a Renish Modular Raman spectrometer equipped with a Stellar Pro Argon-ion laser at 514 nm (50 mW). The crystalline structure was determined by X ray diffraction (XRD) (XRD-7000, Shimazduo) and the surface elemental composition by X-ray photoelectron spectroscopy (XPS) (Krato-ultra DLD, Shimazduo) using Mono Al Ka radiation (hn = 1486.7 eV). The contact angle of water on the material surface was examined by a contact angle meter (JC2000D, China) with a water drop volume of 0.2 μL.

Liner sweep voltammetry (LSV) was carried out to compare the electrochemical behavior during H_2O_2 generation, which were recorded by the CHI660D workstation at a scan rate of 50 mV s^{-1} in a three-electrode cell system. The modified cathode was used as the working electrode, a platinum sheet as the counter electrode and a saturated calomel electrode (SCE) as the reference electrode at ambient temperature. Electrochemical impedance spectroscopy (EIS) were performed in the frequency range of 0.1-10^5 Hz. The specific surface area of the electrodes was determined by nitrogen adsorption in a constant volume adsorption apparatus (BET, Autosorb-UQ-MP, America). What's more, cyclic voltammogram (CV) was used to explore the ORR activity for H_2O_2 generation on the modified and unmodified

View Article Online
DOI: 10.1039/C7TA01534H

graphite felt cathodes. And the active surface area of the electrodes, rotating disk electrode (RDE) was used to investigate the oxygen reduction activity of modified electrode in saturated O_2 solution at a scan rate of 50 mV s^{-1}.

Different kinds of cathodes with or without EEGr were made for the RDE study, respectively. For the carbon black electrode, 7 mg carbon black with 0.9 mL ethanol and 0.1 mL PTFE was mixed, and to prepare for another working electrode, 2 mg EEGr and 8 mg carbon black powder was suspended in a mixture containing 0.9 mL ethanol and 0.1 mL PTFE, after the quick shock for 10 s, 0.01 mL of the mixture was dropped onto a glass carbon electrode (0.196 cm^2) and then dried at room temperature.

The selectivity for H_2O_2 production was evaluated by the calculation of the electron transfer numbers according to the slopes of the Koutecky-Levich plots by the following two equations:[27]

$$\frac{1}{J} = \frac{1}{J_k} + \frac{1}{Bw^{\frac{1}{2}}} \tag{5}$$

$$B = 0.62nFAv^{\frac{1}{6}}C_{o_2}D_{o_2}^{\frac{2}{3}} \tag{6}$$

Where J and J_k are the detected current density and kinetic current density, respectively (mA cm^{-2}), w is the angular velocity (rad s^{-1}), F is the Faraday constant (C mol^{-1}), n is the electron transfer numbers, C_{o_2} is the bulk concentration of O_2 (mol cm^{-3}), v is the kinematic viscosity (cm^2 s^{-1}), and D_{o_2} is the diffusion coefficient of O_2 in the electrolyte solution (cm^2 s^{-1}).

In order to ensure the electroactive surface area of the modified graphite felts, the Randles-Sevcik equation was used as follows:[28,29]

View Article Online
DOI: 10.1039/C7TA01534H

$$I_P = 2.69\times10^5 \times AD^{\frac{1}{2}} n^{\frac{1}{2}} \upsilon^{\frac{1}{2}} C \quad (7)$$

Where I_P is the peak current (A), n is the number of electrons involving in the redox reaction (n=1), A is the area of the electrode (cm^2), D is the diffusion coefficient of the molecule in solution (7.6×10^{-6} cm^2 s^{-1}), C is the concentration of the probe molecule in the bulk solution (1×10^{-5} cm^3) and *v* is the scan rate of the CV (0.01 V s^{-1}).

Pollutants degradation by electro-Fenton

In order to verify the performance of cathodes, the graphite felts modified with or without EEGr were used as the cathode for pollutants degradation by electro-Fenton. The electrolyte solution was same as the one for H_2O_2 generation except the addition of 0.04 mM $FeSO_4$.

Antibiotics are widely used in humans and animals to prevent and treat infection diseases, dyes and phenols are widely presented in many industries wastewater,[30,31] thus Orange II (50 mg L^{-1}), methylene blue (50 mg L^{-1}), phenol (50 mg L^{-1}) and sulfadiazine (20 mg L^{-1}) were chosen as the representative pollutants. The concentration and Total organic carbon (TOC) removal efficiency of each pollutant were detected every 10 min intervals and the results with the two cathodes were compared with each other.

TOC was monitored by a TOC analyzer (Analytikjena multi N/C 3100, Germany) to qualify the degree of mineralization in the electro-Fenton treatment of pollutants. The concentration removal efficiency (R%) and TOC removal efficiency (TOC%) of the pollutants were calculated according to the following equations, respectively:

View Article Online
DOI: 10.1039/C7TA01534H

$$R(\%) = \frac{c_0 - c_t}{c_0} \times 100\% \quad (8)$$

$$TOC\% = \frac{TOC_0 - TOC_t}{TOC_0} \times 100\% \quad (9)$$

Where c_0, TOC_0, c_t, TOC_t was the initial and final value of pollutants concentration and TOC, respectively.

Results and discussion

The SEM image (Fig. 1a) revealed that the EEGr flakes were thin sheets, and all of them were laminar arrangement. The TEM image reconfirmed they were 3-4 thin laminar layers (Fig. 1b and 1c). The typical AFM image (Fig. 1d) showed that, the statistical thickness of the EEGr flakes were within 3 nm. As we known, the single sheet graphene was 0.7-1.0 nm,[32] so it could be concluded that the synthesized graphene was 3-4 layers, which was consistent with TEM observation.

Fig. 1e shows Raman spectrum of EEGr and the original graphite foil. The bands of 1350 and 1582 cm^{-1} represented the D and G bands, respectively. Obviously the EEGr exhibited an intense D bond, where graphite foil didn't have. It was reported that D band had relation with the disorder or defect in the structure because of the disorderliness in the graphene sheets.[33] Besides, the D/G value was 0.52, which was similar to the result of 0.54 reported by Chen et al.,[34] and was much smaller than the reduced graphene oxide (1.0-1.5),[35] suggesting that a low defect density of EEGr was obtained. What's more, the EEGr had an intense 2D bond at around 2720 cm^{-1}, which was the evidence of sp^2 carbon materials, and 2D/G ratio was assigned to a second

View Article Online
DOI: 10.1039/C7TA01534H

order two phonon process and usually used to determine the layers of graphene.[36] The 2D/G ratio of 0.76 showed that the 4 layer numbers of EEGr had low defects and few layer numbers.

(Fig. 1)

The XRD pattern of graphite foil and EEGr (Fig. 2a) displayed that the two materials had a strong sharp diffraction peak (002) and a weaker sharp peak (004), which were attributed to the crystalline graphitic strctuce.[20,37] It should be noted that the highest intensity peak (002) for EEGr was found to be shifted toward the lower diffraction angles (26.42°), which was 26.76° for graphite foil. The results proved that the lattice was expanded during electrochemical exfoliation.[36]

XPS presented the chemical composition of the EEGr and graphite foil (Fig. 2b): the atomic oxygen content detected in EEGr and graphite foil was 12.88% and 8.52%, and the atomic carbon content was 81.69% and 89.49%, respectively (Table 1). The measured O/C atomic ratios thus increased from 0.095 (graphite foil) to 0.157 (EEGr), which were higher than others,[34,38] but still lower than 0.18 derived from anodic exfoliation.[35] According to the high-resolution spectrum of C 1s (Fig. 2c and Fig. 2d), a sharp peak existed at a binding energy (BE) of 284.8 eV corresponding to the sp^2 carbon (graphitic C=C species), and the other peaks at 285 eV, 286.3 eV and 287.2 eV are assigned to the sp^3 carbons (C-OH), and the carbon-oxygen groups (C-O-C, C=O), respectively.[19,38] Compared to graphite foil, the intensity of C-OH peak of EEGr

View Article Online
DOI: 10.1039/C7TA01534H

increased a little and the C=O peak was detected in EEGr while not in graphite foil, which confirmed that part of the graphite foil was oxidized in the process of synthesis graphene.

(Fig. 2)

(Table 1)

Optimizing the ratio and loading of EEGr on modified graphite felt cathode

The ratio and loading of EEGr on graphite felt would significantly affect the cathode characteristics and its performance for hydrogen peroxide production, thus they were optimized as two important factors in cathode manufacture. Fig. 3a shows the yield of H_2O_2 on the cathodes modified with different ratio of EEGr to carbon black (0, 10, 20, 30, 40%). It was observed that the concentration of H_2O_2 after 60 min electrolysis increased with the increase of EEGr ratio until 20%, but further increase the ratio led to the decrease of H_2O_2. For cathode modified with 20% EEGr (for simplification, we called it EGGr-20), the concentration of H_2O_2 reached near 100 mg L^{-1}, which was much higher than the unmodified (EEGr-0). Accordingly, EEGr-20 obtained the highest H_2O_2 production rate with the lowest EEC of 5.2 kWh kg^{-1} (insert Fig. 3a).

The EEGr synthesis process was further optimized with different loadings of EEGr when all ratios held on 20%. As shown in Fig.3b, a higher EGGr loading enhanced the H_2O_2 production, and the highest H_2O_2 production was obtained with EEGr loading of 0.056 g, which was almost no difference with that of EEGr loading of 0.072g and

View Article Online
DOI: 10.1039/C7TA01534H

more than 1.5 times of the unmodified one. According to these experimental results, the EEGr ratio of 20% with loading of 0.056 g (i.e., 11.2 mg cm^{-2}) was chosen as the proper condition.

(Fig. 3)

Performance and stability of the modified cathode for H_2O_2 production

To explore the proper cathode potential, the yield of H_2O_2 at -0.5, -0.7, -0.9 and -1.1 V were investigated. As shown in Fig. 4a, it increased with the improvement of cathode potential, reaching 426 mg L^{-1} (- 1.1 V) at 120 min. The CE followed the same tendency with cathode potential (insert Fig. 4a), which was in agreement with literature.[39] However, EEC was found significantly increased with cathode potential. Taking these factors into consideration, it could be concluded that -0.9 V was the optimized condition, in which the average H_2O_2 generation rate was 3.7 mg h^{-1} cm^{-2}, which was more than 3 times of the one in a graphene doped gas diffusion electrode (GDE).[5]

H_2O_2 generation is dependent on pH value due to the participation of proton in H_2O_2 electro-generation process.[40] The results in Fig. 4b showed that the yield of H_2O_2 was the highest at pH 7, and then decreased as pH continued to increase, which was 366 mg L^{-1} at pH 9 and 336 mg L^{-1} at pH 11 with average H_2O_2 generation rate of 7.5 and 7.2 mg h^{-1} cm^{-2}. These facts proved that pH 7 was the proper condition for H_2O_2 generation, which was accordant with literatue.[15] One possible reason was that the residual H^+ reduced at the cathode with H_2 generation might be a competing

View Article Online
DOI: 10.1039/C7TA01534H

reaction that decreased H_2O_2 generation.[41-43] Since the conversion of dissolved oxygen to H_2O_2 consumes protons in acidic solution,[43] according to eq. 1 (Line 53). The decrease of H_2O_2 at high pH condition was because that the H^+ existed in the solution may be not enough for the generation of H_2O_2, leading to a lower yield of H_2O_2 at pH 9 and 11. Additionally, the inset Fig. 4b also proved that the highest yield of H_2O_2 was obtained at pH 7 with the highest current efficiency and the lowest energy consumption.

Fig. 4c shows the repeated experiments operated over 10 consecutive batches using the same modified cathode under the same conditions. After 10 cycles, the average rate of H_2O_2 generation slightly fluctuated around 7.2 mg h^{-1} cm^{-2}, and all of the EEC were around 9.7 kWh kg^{-1}, indicating that the modified graphite felt cathode with EEGr was pretty stable and reusable for the production of H_2O_2 with a low energy consumption.

(Fig. 4)

The performances (H_2O_2 production rate, EEC and CE) of the modified graphite felt cathodes in this study were compared with literature that using graphene, or the most common graphite felt and GDE as the cathode (Table 2). Compared with all the reported cathode using graphene or graphene coating/doping, the H_2O_2 production rate in the present work was the highest, though some EEC and EC data were not available. For example, Xu et al. used graphene doped GDE for the degradation of

View Article Online
DOI: 10.1039/C7TA01534H

brilliant blue with a H_2O_2 generation rate of 1.03 mg h^{-1} cm^{-2},[5] and Mousset et al. reported that 0.0048, 0.0072 and 0.64 mg h^{-1} cm^{-2} were obtained with graphene coated on quartz, graphene sheet, and 3D graphene foam cathode.[20] In the present work, even at low bias potential of -0.5 V, the H_2O_2 generation rate could reach 1.3 mg h^{-1} cm^{-2}.

Compared with the modified cathodes using graphite felt as the base, the modification with graphene in the present work also possessed the best performance. For example, H_2O_2 generation rate of 0.44 and 1.4 mg h^{-1} cm^{-2} was obtained with the modification of carbon-PTFE and anodization, respectively.[44,45] In our previous work, the H_2O_2 generation rate on the graphite felt modified with carbon black increased to 2.2 mg h^{-1} cm^{-2},[15] but the energy consumption (7.5 kWh kg^{-1}) was much higher than that in the present work (4.9 kWh kg^{-1}).

Generally, GDE is regarded as one of the best type of cathode for H_2O_2 production, which is also verified in Table 2, in which the H_2O_2 generation rate advantage over graphite felt based electrodes. However, this high H_2O_2 generation rates are usually accompanied by high EEC. For example, Reis et al. obtained a 11 mg h^{-1} cm^{-2} H_2O_2 generation rate with a high EEC of 22.1 kWh kg^{-1} due to the high potential of -1.75 V.[46] Therefore, if taken account for the same EEC, this result was still worse than the result the present work (7.7 mg h^{-1} cm^{-2} H_2O_2 generation rate with a EEC of 9.7 kWh kg^{-1}).

In summary, the results proved that modified graphite felt cathode with EEGr in this study was outstanding for the ultrahigh generation rate of H_2O_2 with relatively low EEC at the same time, which would be more promising for practical application.

View Article Online
DOI: 10.1039/C7TA01534H

(Table 2)

Possible mechanism for the high yield of H_2O_2 production

To discover why this modified cathode have a very high yield of hydrogen peroxide production, many characterizations were carried out. Fig. 5a shows the nitrogen adsorption isotherms of EEGr-20 and unmodified graphite felt cathode. The BET surface area and pore volume of unmodified graphite felt were 3.92 m^2 g^{-1} and 0.0026 cm^3 g^{-1}, while 9.83 m^2 g^{-1} and 0.029 cm^3 g^{-1} for EEGr-20 cathode. The results suggested that EEGr-20 cathode reached about 2.5 times and 11.2 times of BET and pore volume of the unmodified graphite felt cathode, respectively. Such significant improvement would be of great advantage to enhance the yield of H_2O_2.

The conductivity of EEGr-20 and unmodified graphite felt electrodes can be confirmed by EIS. Fig. 5b shows that each Nyquist plot includes a semicircle part and a liner part. The semicircle is an indication of the charge transfer resistance during the electrochemical reaction and the line can be attributed to the diffusion controlled Warburg impedance.[50] The results showed that EIS of unmodified graphite felt electrode has a larger semicircle and tilted vertical line in low frequency region. By contrast, the EEGr-20 electrode consists of a slightly depressed semicircle in high frequency and more vertical line in the range of low frequency, indicating that EEGr-20 electrode has lower charge transfer resistance and faster ion diffusion compared with unmodified graphite felt electrode. Thus it can be concluded that the

View Article Online
DOI: 10.1039/C7TA01534H

EEGr has contributed to the high electrochemical performance of EEGr-20 electrode.

Fig. 5c shows CV of the three different cathodes (EEGr-0, EEGr-20 and unmodified graphite felt cathode), confirming EEGr-20 had the highest peak current density. It was observed that EEGr-20 had a strong reduction peak at -0.4 V vs SCE, proving a fast reduction rate for H_2O_2 production on the cathode.[28,39]

RDE was further used to investigate the ORR activity of the modified cathode, as shown in Fig. 5d and Fig. 5e, the current density increased with rotation rate because of the shortened diffusion layer,[51] which was consistent with literature.[27] The curves of steady-state diffusion plateau currents analyzed through Koutecky-Levich plots (inset in Fig. 5d and Fig. 5e) proved the electron number during the electrochemical processes, which was 2.25 (EEGr-0) and 2.43 (EEGr-20), showing both processes with the two electrodes were two-electron ORR processes. Therefore, EEGr introduction simply accelerated the rate of the electron transfer rather than changing the ORR mechanism, which was consistent with the results of H_2O_2 production in Fig. 3a and Fig.3b.

Additionally, CV of the modified graphite felts were operated in solution of $[Fe(CN)_6]^{3-}/[Fe(CN)_6]^{4-}$ (Fig. 5f), and a 1.5-fold increase of the peak current was observed on EEGr-20, proving that the introduction of EEGr could improve the active surface of the modified electrode. According to eq. 7, the electroactive surfaces were calculated to be 171 cm^2 (EEGr-20) and 116 cm^2 (EEGr-0). The 1.5-fold improvement of the surface area should lead to a higher rate of electrochemical reactions on the cathode, which was consistent with the results in Fig. 5c.

View Article Online
DOI: 10.1039/C7TA01534H

The contact angles were commonly used to measure the hydrophilicity of carbon materials. Hydrophilicity is a critical feature for H_2O_2 generation, generally, the higher hydrophilicity, the faster diffusion of O_2, and thus result in a higher H_2O_2 generation.[28] From Fig. 5g to Fig. 5i, the contact angles of three different cathodes were presented, which were 123° (unmodified graphite felt), 112° (modified graphite felt with EEGr-0) and 100° (modified graphite felt with EEGr-20), respectively. It can be seen that the hydrophilicity of modified cathode with EEGr-20 was highest, providing helpfulness to O_2 diffusion and high yield of H_2O_2 production.

(Fig. 5)

Based on the characterizations above, a possible mechanism for this ultrahigh production of hydrogen peroxide is suggested. Fig. 6 shows the schematic diagram of the ORR on the modified graphite felts with/without EEGr. The introduction of EEGr on the cathode not only accelerated the rates of electrons transfer without changing the mechanism of ORR, but also increased the cathode surface hydrophilicity to promote oxygen diffusion. What's more, the electroactive surface of cathode was also improved, which increased active site on the cathode for ORR. These factors contributed to a higher H_2O_2 production with a lower EEC.

(Fig. 6)

View Article Online
DOI: 10.1039/C7TA01534H

The performance of pollutants degradation

In order to evaluate the effectiveness of the modified cathode with EEGr-20 for electro-Fenton, the degradation of a series of model organic pollutants including orange II, methylene blue, sulfadiazine and phenol were conducted. As shown in Fig. 7, almost all of the pollutants could be completely removed within 1 h, and the removal efficiencies on EEGr-20 were much better than that on EEGr-0. Their difference on TOC removal was more significant (insert Fig. 7), for example, the TOC removal efficiency of sulfadiazine was about 100% on EEGr-20, while only about 69% for EEGr-0. Table 3 lists the comparison of pollutant and TOC removal efficiency, as well as the pseudo-first order kinetic constant (*k*). The results proved that about 1.95-2.47 fold of the *k* value were obtained with EEGr-20 compared with the ones with EEGr-0. This phenomenon was not surprised since it was consistent with the results of H_2O_2 production, proving that the modified cathode with EEGr-20 was potent for organic wastewater treatment by electro-Fenton.

(Fig. 7)

(Table 3)

Conclusions

A novel modified graphite felt cathode with graphene by electrochemical exfoliation method was developed, which presented an ultrahigh yield of H_2O_2 production. The EEGr was proved to be 3-4 layers with low level defects. Optimized ratio of EEGr

View Article Online
DOI: 10.1039/C7TA01534H

and loading on the modified graphite felts were explored, and EEGr-20 with a loading of 11.2 mg cm^{-2} was the best for H_2O_2 production. By optimizing cathode potential and pH, a significant improvement of H_2O_2 yield of 7.7 mg h^{-1} cm^{-2} was obtained at pH 7 and -0.9 V potential. In addition, this performance kept stable after 10 cycles reuse. Possible mechanism for this high performance was suggested. Finally, the model pollutants degradation confirmed the great potential practical application for organic wastewater treatment by electro-Fenton.

Acknowledgments

This work was financially supported by National Key Research and Development Program (2016YFC0400706), Key Project of Natural Science Foundation of Tianjin (no. 16JCZDJC39300), Natural Science Foundation of China (no. 21273120 and 51178225), China National Water Project (no. 2015ZX07203-11), and Fundamental Research Funds for the Central Universities.

Notes and references

1 J. M. C. -Martin, G. B. -Brieva and J. L. G. Fierro, Angew. Chem. Int. Edit., 2006, 45, 6962 – 6984.

2 P. Biasi, F. Menegazzo, P. Canu, F. Pinna and T. O. Salmi, Ind. Eng. Chem. Res., 2013, 52, 15472−15480.

3 I. Huerta, P. Biasi, J. G. -Serna, M. J. Cocero, J. P. Mikkola and T. Salmi, Catal. Today, 2015, 248, 91–100.

4 D. Johinke, S. P. D. Graaf and R. Bathgate, Anim. Reprod. Sci, 2014,151, 208–219.

View Article Online
DOI: 10.1039/C7TA01534H

5 X. C. Xu, J. Chen, G. Q. Zhang, Y. Song and F. L. Yang, Int. J. Electrochem. Sc., 2014, 9, 569-579.

6 G. S. Xia, Y. H. Lu and H. B. Xu, Separation and Purification Technology, 2015, 156, 553–560.

7 M. Pimentel, N. Oturan, M. Dezotti and M. A. Oturan, Appl. Catal. B-Environ., 2008, 83, 140–149.

8 A. Özcan, Y. Sahin¸ A. S. Koparal and M. A. Oturan, J. Hazard. Mater, 2008, 153, 718–727.

9 M. Panizza and M. A. Oturan, Electrochim. Acta, 2011, 56, 7084–7087.

10 J. Liu, X. J. Sun, P. Song, Y. W. Zhang, W. Xing and W. L. Xu, Adv. Mater., 2013, 25, 6879–6883.

11 A. Thiam, M. H. Zhou, E. Brillas and I. Sirés, Appl. Catal. B-Environ., 2014, 150–151, 116–125.

12 Y. Shiraishi, Y. Kofuji, H. Sakamoto, S. Tanaka, S. Ichikawa and T. Hira. Acs. Catal., 2015, 5, 3058-3066.

13 T. F. Liu, K. Wang, S. Q. Song, A. Brouzgou, P. Tsiakaras and Y. Wang, Electrochim. Acta, 2016, 194, 228–238.

14 J. F. Carneiro, M. J. Paulo, M. Siaj, A. C. Tavares and M. R.V. Lanza, J. Catal., 2015, 332, 51–61.

15 F. K. Yu, M. H. Zhou and X. M. Yu, Electrochim. Acta, 2015, 163, 182–189.

16 X. X. Chen and B. L. Chen, Environ. Sci. Technol., 2015, 49, 6181-6189.

17 C. Domínguez, F. J. P. -Alonso, M. A. Salam, S. A. A. -Thabaiti, M. A. Peña, L.

View Article Online
DOI: 10.1039/C7TA01534H

Barrio and S. Rojas, J. Mater. Chem. A, 2015, 3, 24487–24494.

18 L. Liu, L. H. Liao, Q. H. Meng and B. Cao, Carbon, 2015, 90, 75–84.

19 T. X. H. Le, M. Bechelany, J. Champavert and M. Cretin, Rsc. Adv., 2015, 5, 42536–42539.

20 E. Mousset, Z. X. Wang, J. Hammaker and O. Lefebvre, Electrochim. Acta, 2016, 214, 217-230.

21 C. Y. Chen, C. Tang, H. F. Wang, C. M. Chen, X. Y. Zhang, X. Huang and Q. Zhang, Chemsuschem, 2016, 9, 1194 –1199.

22 Y. R. Leroux, J. -F. Bergamini, S. Ababou, J. -C. L. Breton and P. Hapiot, J. Electroanal. Chem., 2015, 753, 42–46.

23 J. H. Lopes, S. Ye, J. T. Gostick, J. E. Barralet and G. Merle, Langmuir, 2015, 31. 9718-9727.

24 E. Mousset, Z. T. Ko, M. Syafiq, Z. X. Wang and O. Lefebvre, Electrochim. Acta, 2016, 222, 1628-1641.

25 Z. M. Qiang, J. -H. Chang and C. -P. Huang, Water. Res., 2002, 36, 85–94.

26 E. Brillas, I. Sirés and M. A. Oturan, Chem. Rev. 2009, 109, 6570–6631.

27 J. Sun, P. Song, Y. W. Zhang, C. P. Liu, W. L. Xu and W. Xing, Sci. Rep., 2013, 272-277.

28 T. X. H. Le, M. Bechelan, S. Lacour, N. Oturan, M. A. Oturan and M. Cretin, Carbon, 2015, 94, 1003–1011.

29 Y. S. Grewal, M. J. A. Shiddiky, S. A. Gray, K. M. Weigel, G. A. Cangelosi and M. Trau, Chem. Commun., 2013,49, 1551-1553.

View Article Online
DOI: 10.1039/C7TA01534H

30 J. F. Yang, S. B. Zhou, A. G. Xiao, W. J. Li and G. G. Ying, J. Environ. Sci. Heal. B, 2014, 49, 909–916.

31 W. L. Yang, H. X. Han, M. H. Zhou and J. Yang, Rsc. Adv., 2015, 5, 49513–49520.

32 W. H. Duan, K. Gong and Q. Wang, Carbon, 2011, 49, 3107 – 3112.

33 C. -Y. Su, A. -Yu. Lu, Y. P. Xu, F. -R. Chen, A. N. Khlobystov and L. -J. Li, Nanoscale, 2011, 3, 2332-2339.

34 C. -H. Chen, S. -W. Yang, M. -C. Chuang, W. -Y. Woon and C. -Y. Su, Nanoscale, 2015, 7, 15362–15373.

35 J. M. Munuera, J. I. Paredes, S. V. -Rodil, M. A. -Varela, A. Pagán, S. D. A. -Cervantes, J. L. Cenis, A. M. -Alonso and J. M. D. Tascón, Carbon, 2015, 94, 729–739.

36 N. Mahato, N. Parveen and M. H. Cho, Mater. Express, 2015, 5, 471-479.

37 J. X. Guo, T. Zhang, C. G. Hu and L. Fu, Nanoscale, 2015, 7, 1290–1295.

38 S. Yang, S. Bruller, Z. -S. Wu, Z. Y. Liu, K. Parvez, R. H. Dong, F. Richard, P. Samorì, X. L. Feng and K. Mullen, J. Am. Chem. Soc., 2015, 137, 13927-13932.

39 G. S. Xia, Y. H. Lu and H. B. Xu, Electrochim. Acta, 2015, 158, 390–396.

40 Y. M. Liu, S. Chen, X. Quan, H. T. Yu, H. M. Zhao and Y. B. Zhang, Environ. Sci. Technol., 2015, 49, 13528-13533.

41 B. G. Kwon, D. S. Lee, N. Kang and J. Yoon, Water. Res., 1999, 33, 2110-2118.

42 M. Panizza and G. Cerisola, Water. Res., 2009, 43, 339-344.

43 C. -T. Wang, J. -L. Hu, W. -L. Chou and Y. M. Kuo, J. Hazard. Mater, 2008, 152, 601-606.

View Article Online
DOI: 10.1039/C7TA01534H

44 L. Zhou, M. H. Zhou, C. Zhang, Y. H. Jiang, Z. H. Bi and J. Yang, Chem. Eng. J., 2013, 233, 185–192.

45 A. D. Pozzo, L. D. Palma, C. Merli and E. Petrucci, J. Appl. Electrochem., 2005, 35, 413-419.

46 R. M. Reis, A. A. G. F. Beati, R. S. Rocha, M. H. M. T. Assumpao, M. C. Santos, R. Bertazzoli and M. R. V. Lanza, Ind. Eng. Chem. Res., 2012, 51, 649–654.

47 R. B. Valim, R. M. Reis, P. S. Castro, A. S. Lima, R. S. Rocha, M. Bertotti and M. R. V. Lanza, Carbon, 2013, 61, 236 – 244.

48 X. M. Yu, M. H. Zhou, G. B. Ren and L. Ma, Chem. Eng. J., 2015, 263 , 92–100.

49 E. Mousset, Z. X. Wang, J. Hammaker, O. Lefebvre, Electrochim. Acta, 2016, 214, 217–230.

50 S. Khamlich, T. Khamliche, M. S. Dhlamini, M. Khenfouch, B. M. Mothudi and M. Maaza, J. Colloid. Interf. Sci, 2017, 493, 130-137.

51 W. Yang, T. -P. Fellinger and M. Antonietti, J. Am. Chem. Soc., 2011, 133, 206–209.

View Article Online
DOI: 10.1039/C7TA01534H

Figure captions

Fig. 1 SEM (a), TEM (b, c) and AFM (d) of the EEGr from the graphite foil, Raman spectrum of graphite foil and EEGr (e).

Fig. 2 XRD patterns of the graphite foil and EEGr (a); XPS spectra of graphite foil and EEGr (b); high-resolution C 1s spectrum of EEGr (c) and graphite foil (d).

Fig. 3 The performances of modified graphite felts with different ratio (a) and loading of EEGr (b) for H_2O_2 generation.

Fig. 4 The performance of H_2O_2 generation with different potentials (a) and pH (b); Stability of modified cathode with EEGr-20 over 10 cycles of the rate of H_2O_2 generation and EEC (c). Conditions: V=100 mL, pH=7, Potential: -0.9 V.

Fig.5 N_2 adsorption/desorption isotherms of EEGr-20 and unmodified graphite felt electrodes (a); Nyquist plot of EEGr-20 and unmodified graphite felt electrodes (b); Cyclic voltammograms of three different modified cathodes (modified graphite felt with EEGr, EEGr-0, EEGr-20) (c); The Linear sweep voltammetry of modified electrode with EEGr-0 (d) and EEGr-20 (e) in O_2 saturated Na_2SO_4 solution at a scan rate of 50 mV s^{-1} with RDE. Inset: K-L plots at different potentials; electrocatalytic activity towards Fe(III)/Fe(II) redox couple detected with CV techniques (f); Contact angles of unmodified graphite felt (g), modified graphite felt with EEGr-0 (h) and with EEGr-20 (i).

Fig. 6 The schematic diagram of the ORR process.

Fig. 7 The degradation of orange II, methylene blue, sulfadiazine and phenol. Conditions: Pt anode; V=100 mL; pH=3; $[Fe^{2+}]$=0.4 mM; Na_2SO_4: 50 mM; Potential: -0.9 V.

View Article Online
DOI: 10.1039/C7TA01534H

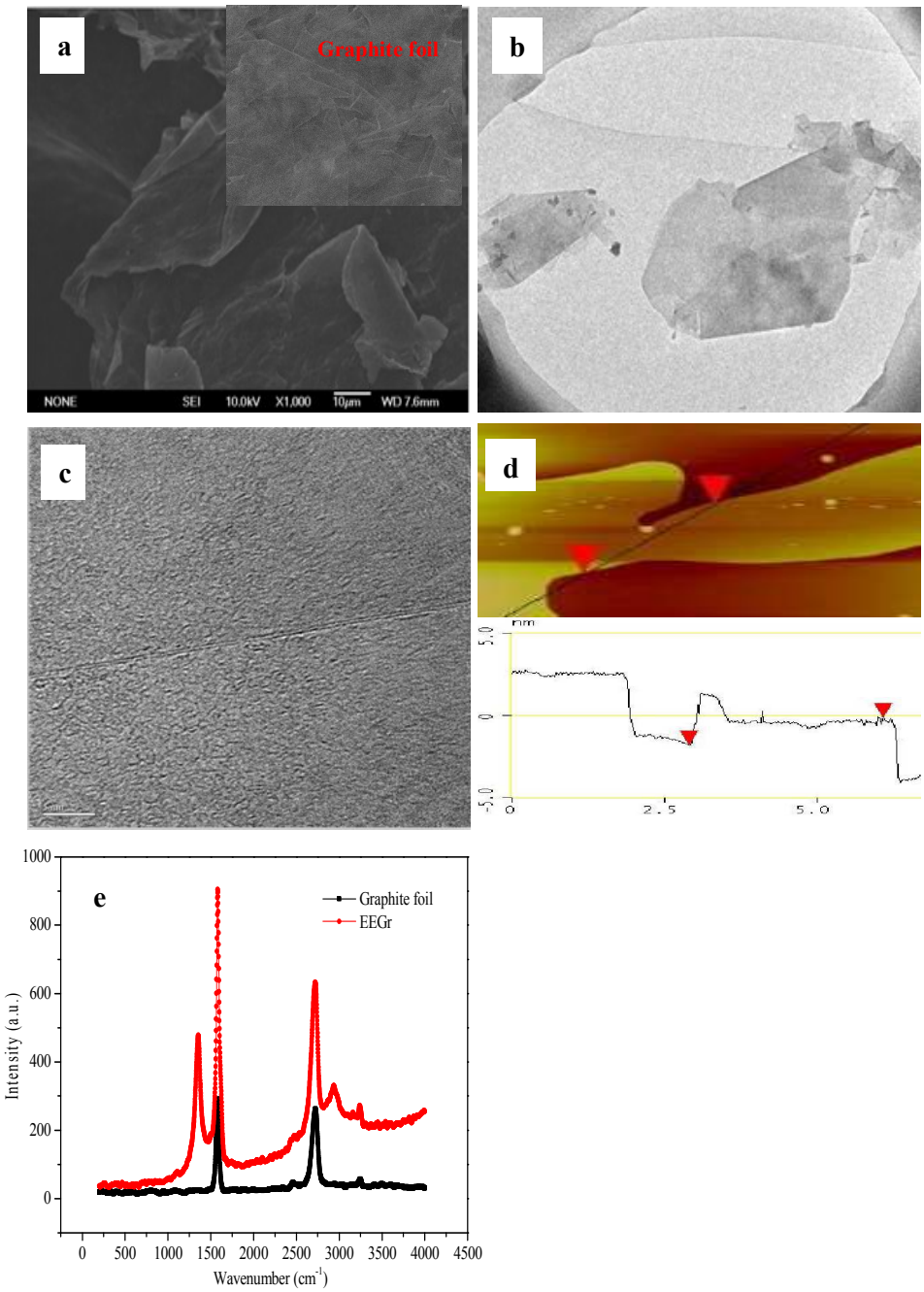

Fig. 1

View Article Online
DOI: 10.1039/C7TA01534H

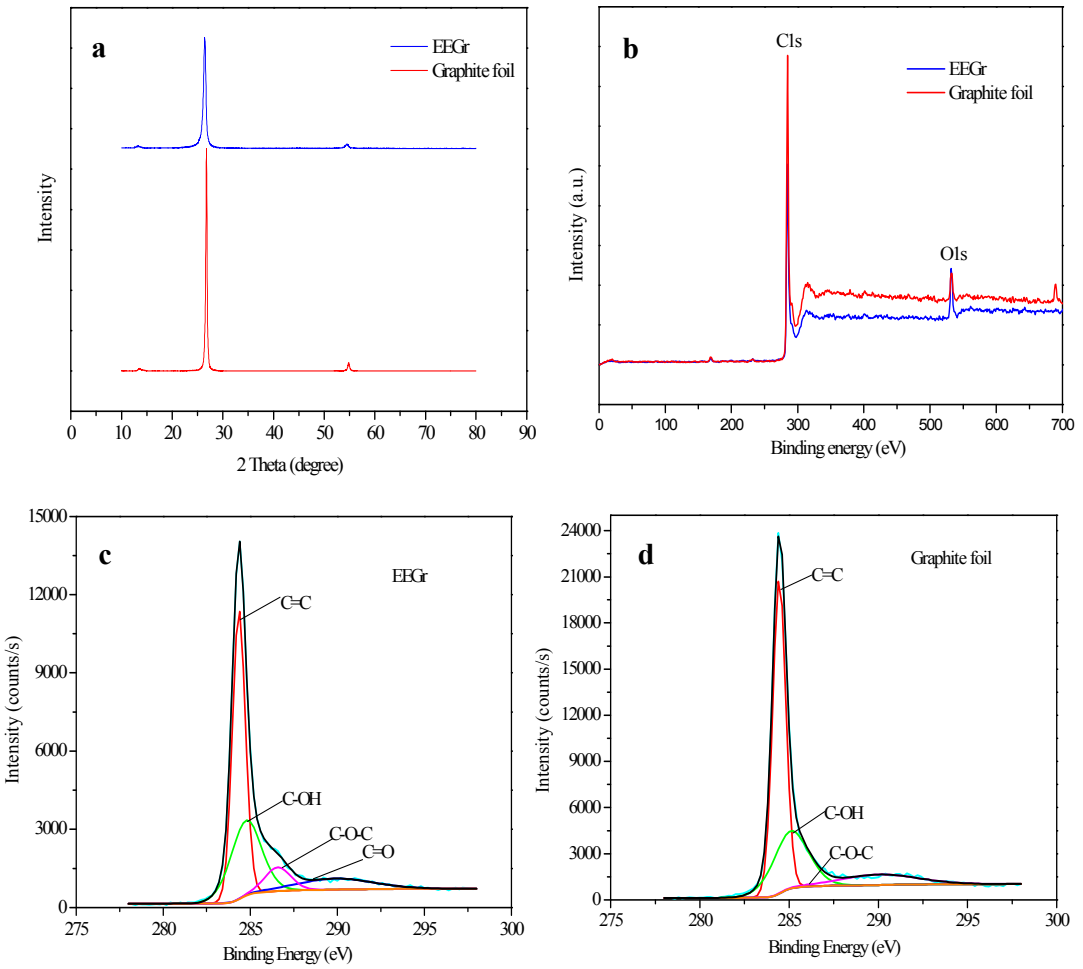

Fig. 2

View Article Online
DOI: 10.1039/C7TA01534H

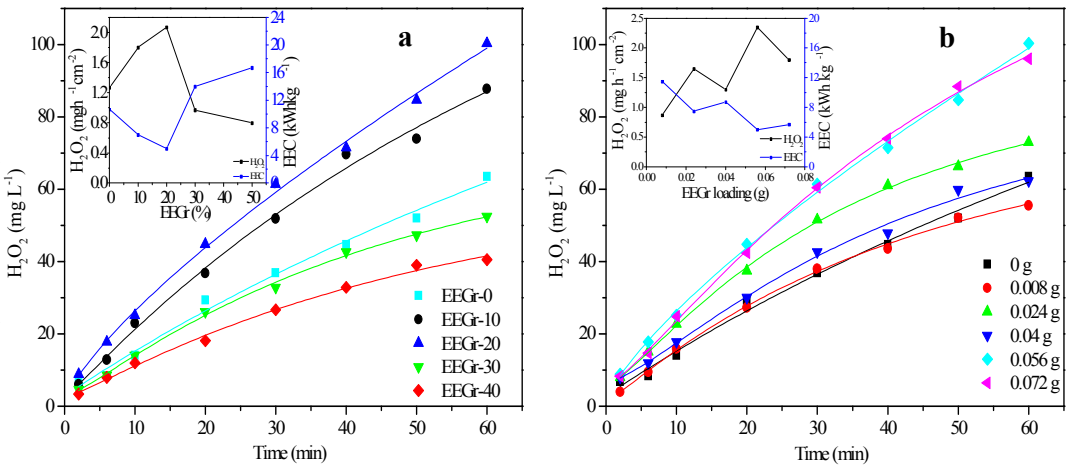

Fig. 3

View Article Online
DOI: 10.1039/C7TA01534H

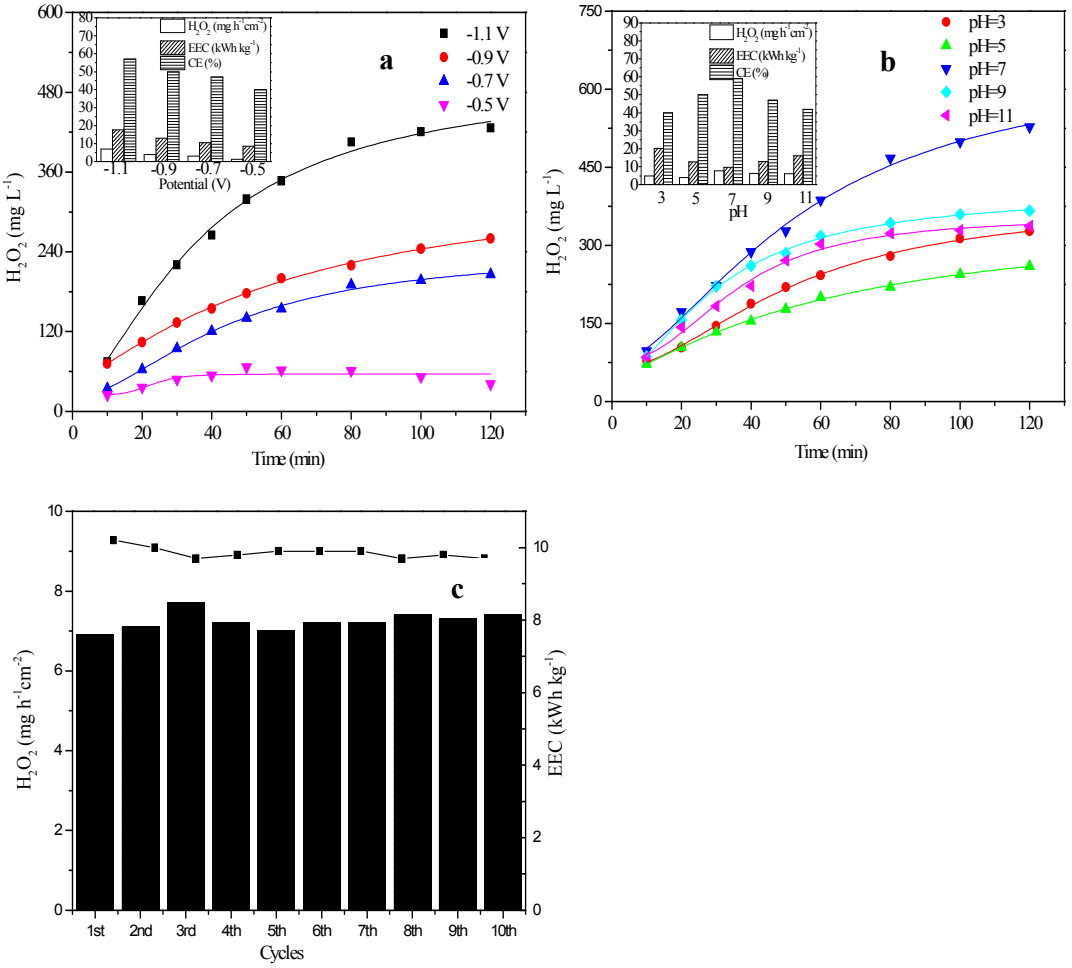

Fig. 4

View Article Online
DOI: 10.1039/C7TA01534H

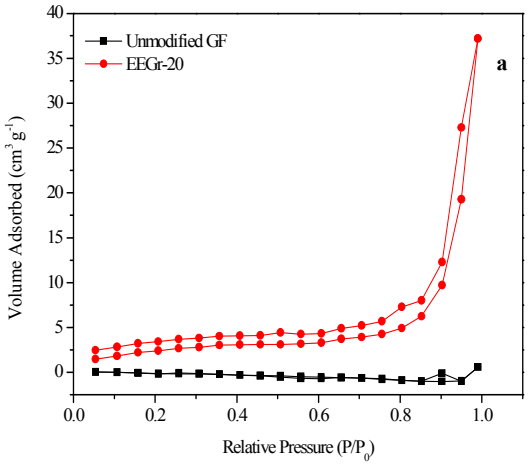

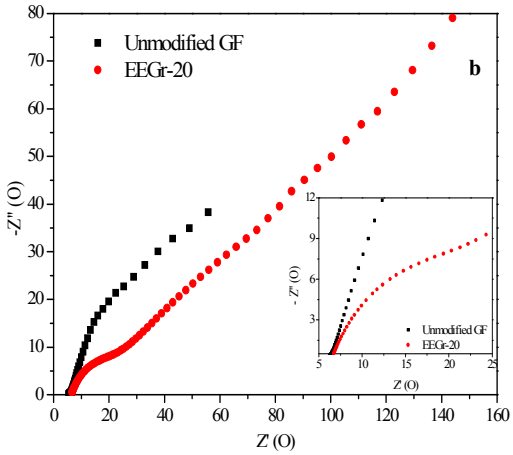

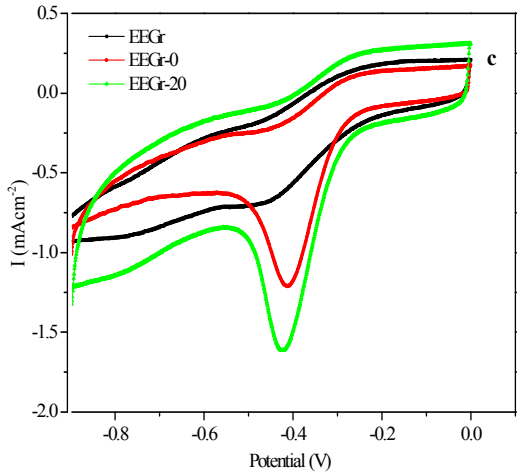

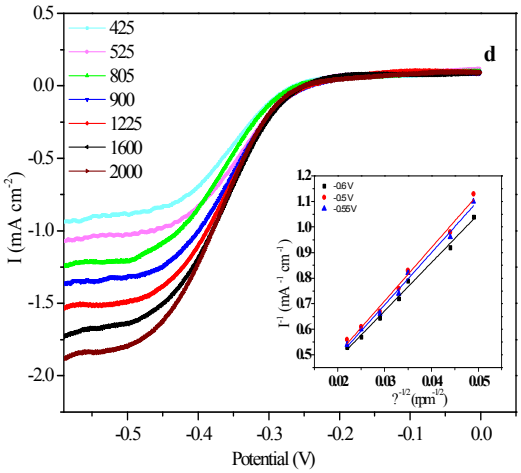

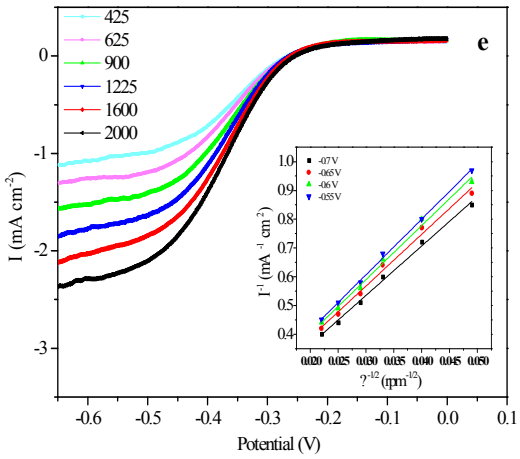

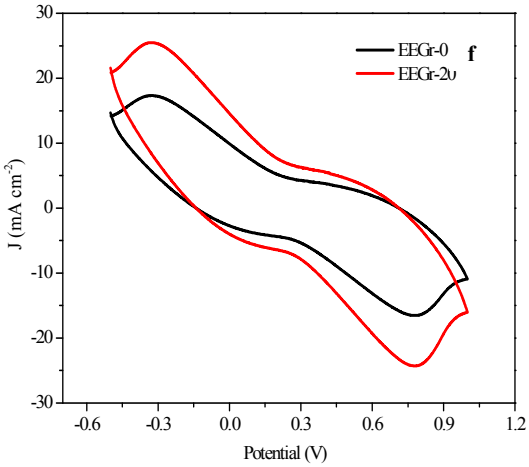

View Article Online
DOI: 10.1039/C7TA01534H

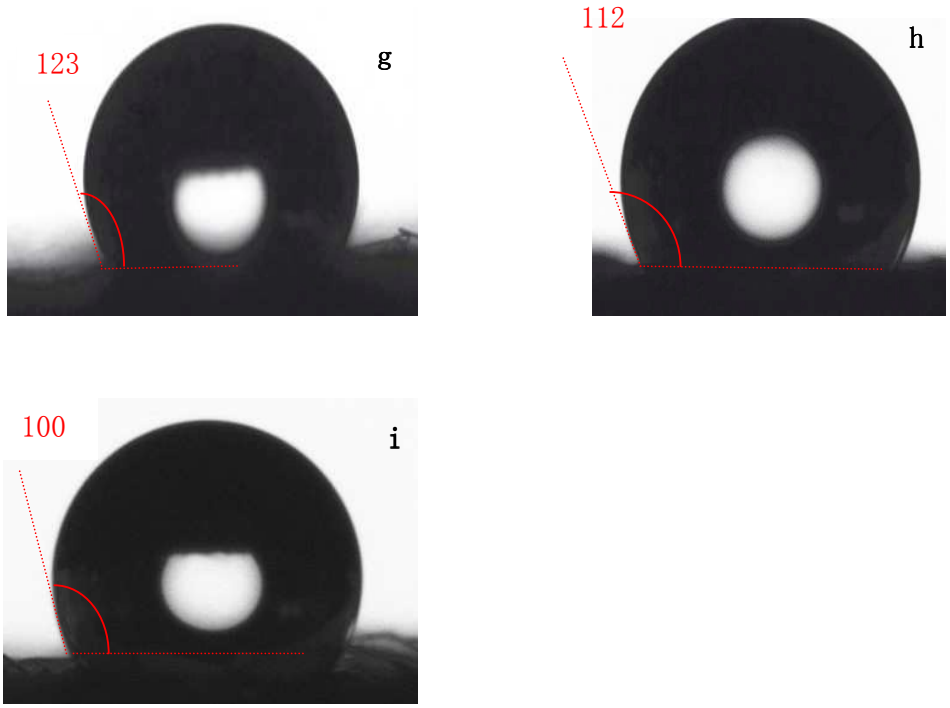

Fig. 5

View Article Online
DOI: 10.1039/C7TA01534H

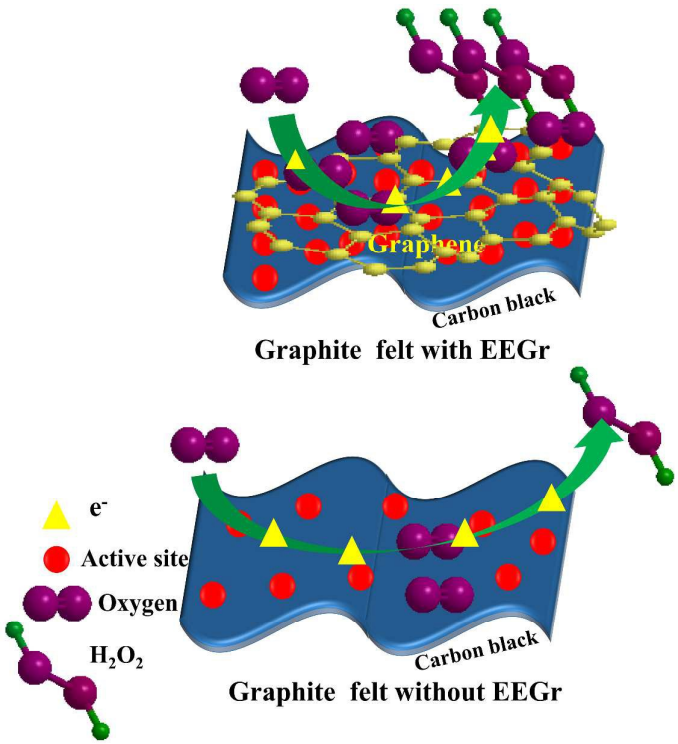

Fig.6

View Article Online
DOI: 10.1039/C7TA01534H

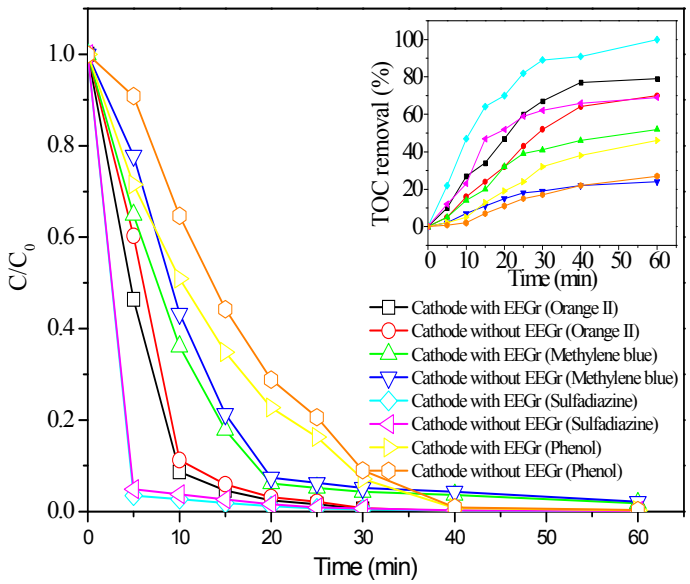

Fig.7

View Article Online
DOI: 10.1039/C7TA01534H

Table 1 Atomic percentage in the samples.

Sample		C1s	O1s	N1s	S2p	O/C
Graphite foil	At %	89.49	8.52	1.27	0.73	0.095
EEGr	At %	81.69	12.88	4.54	0.88	0.157

View Article Online
DOI: 10.1039/C7TA01534H

863 Table 2 Performance comparison with literatures

Cathode material	Experimental conditions	H_2O_2 generation rate (mg h^{-1} cm^{-2})	EEC (kWh kg^{-1})	CE (%)	Reference
Graphite felt modified	Cathode area 3.5 cm^2, V 100 mL, pH 3, O_2 flow rate 0.13 L min^{-1}	1.4	-	35-65	45
Graphite felt modified	Cathode area 10 cm^2, V 130 mL pH 6.4, air flow rate 0.4 L min^{-1}	0.44	-	87	44
Graphite felt modified	Cathode area 20 cm^2, V 100 mL pH 7	2.2	7.5	68-98	15
GDE	Cathode area 20 cm^2, V 400 mL, potential – 1.0 V, O_2 0.02 MPa	4.6	6	-	47
GDE	Cathode area 20 cm^2, V 200 mL, potential – 1.75 V, pH 1, air flow rate 5 L min^{-1}	11	22.1	-	46
GDE	Cathode area 14 cm^2, V 200 mL, pH 7, air flow rate 0.5 L min^{-1}	12.16	15.9	51-88	48
Hierarchically Porous Carbon	Cathode area 10 cm^2, pH 6, bias potential – 0.4 V	/	/	70-90.7	40
Graphite-Graphene	Cathode area 12 cm^2, V 200 mL, pH 3, O_2 flow rate 0.33 L min^{-1}	1.03	6.7	42-68	5
Graphene coated on quartz	Cathode area 20 cm^2, V 150 mL, pH 3, bias potential -0.58 V	0.0048	/	/	
Graphene sheet	Cathode area 20 cm^2, V 150 mL, pH 3, bias potential -0.60 V	0.0072	/	/	20
3D Graphene foam	Cathode area 20 cm^2, V 150 mL, pH 3, bias potential -0.61 V	0.64	/	/	
Carbon cloth-Gr (m_{Gr}: 0.27 mg cm^{-2})	Cathode area 24 cm^2, V 80 mL, pH 3, air flow rate 0.2 L min^{-1}	0.225	/	/	24
Monolayer graphene	V 150 mL, pH 3, bias potential -0.58 V	0.0048	/	/	49
Graphite felt-EEGr (m_{EEGr}: 11.2 mg cm^{-2})	Cathode area 5 cm^2, V 100 mL, pH 5, bias potential -0.5 V	1.3	6.42	67-87	
Graphite felt-EEGr (m_{EEGr}: 11.2 mg cm^{-2})	Cathode area 5 cm^2, V 100 mL, pH 5, bias potential -0.7 V	2.2	4.9	62-92	Present work
Graphite felt-EEGr (m_{EEGr}: 11.2 mg cm^{-2})	Cathode area 5 cm^2, V 100 mL, pH 7, bias potential -0.9 V	7.7	9.7	42-92	

View Article Online
DOI: 10.1039/C7TA01534H

Table 3 Degradation of pollutants with different cathodes.

Pollutants	Cathode	Removal efficiency (%)	TOC (%)	k (min^{-1})	R^2
Orange II	EEGr-20	100	79	0.52	0.98
	EEGr-0	89.8	70	0.22	0.96
Methylene blue	EEGr-20	98.2	52	0.37	0.96
	EEGr-0	88	24	0.19	0.94
Sulfadiazine	EEGr-20	100	100	0.62	0.94
	EEGr-0	87	69	0.27	0.9
Phenol	EEGr-20	95	46	0.37	0.95
	EEGr-0	82	27	0.15	0.90